Construction of Finsler-Lyapunov functions with meshless collocation

Article (Accepted Version)

Construction of Finsler-Lyapunov functions with meshless collocation

Peter Giesl*
Department of Mathematics
University of Sussex
Falmer BN1 9QH
United Kingdom

October 9, 2018

Abstract

We study the stability of invariant sets such as equilibria or periodic orbits of a Dynamical System given by a general autonomous nonlinear ordinary differential equation (ODE). A classical tool to analyse the stability are Lyapunov functions, i.e. scalar-valued functions, which decrease along solutions of the ODE. An alternative to Lyapunov functions is contraction analysis. Here, stability (or incremental stability) is a consequence of the contraction property between two adjacent solutions, formulated as the local property of a Finsler-Lyapunov function. This has the advantage that the invariant set plays no special role and does not need to be known a priori.

In this paper, we propose a method to numerically construct a Finsler-Lyapunov function by solving a first-order partial differential equation using meshless collocation. Depending on the expected attractor, the contraction only takes place in certain directions, which can easily be implemented within the method. In the basin of attraction of an exponentially stable equilibrium or periodic orbit, we show that the PDE problem has a solution, which provides error estimates for the numerical method. Furthermore, we show how the method can also be applied outside the basin of attraction and can detect the stability as well as the stable/unstable directions of equilibria. The method is illustrated with several examples.

Keywords: Dynamical System, stability, Finsler-Lyapunov function, meshfree collocation

1 Introduction

We study the stability of invariant sets such as equilibria or periodic orbits of a Dynamical System given by a general autonomous ordinary differential equation (ODE)

$$\dot{x} = f(x), x \in \mathbb{R}^n. \tag{1}$$

*email p.a.giesl@sussex.ac.uk

A classical tool to analyse the stability are Lyapunov functions. These are scalar-valued functions, which decrease along solutions of the ODE and measure in some way the distance of a point to the invariant set, thus being a global quantity.

A different way of studying stability and the basin of attraction, which does not require any knowledge about the equilibrium and which is also robust with respect to perturbations of the ODE, uses contraction analysis, see [12, 9, 14]; it can be generalised to the study of a Finsler-Lyapunov function [3]. Here, stability is a consequence of the contraction property between two adjacent solutions, so formulated as a local property. This has the advantage that the invariant set plays no special role and does not need to be known a priori.

We search for a Finsler-Lyapunov function of the form[1] $V\colon \mathbb{R}^n \times \mathbb{R}^n \to \mathbb{R}_0^+$, defined on the tangential bundle of the manifold $\mathbb{R}^n$ for every $(x, v) \in \mathbb{R}^n \times \mathbb{R}^n$ which satisfies

$$LV(x,v) := \langle \nabla_x V(x,v), f(x)\rangle + (\nabla_v V(x,v))^T Df(x)v \leq 0, \tag{2}$$

where $\langle \cdot, \cdot \rangle$ denotes the Euclidean scalar product in $\mathbb{R}^n$, as well as the property

$$c_1\|v\|^p \;\; \leq \;\; V(x,v) \;\; \leq \;\; c_2\|v\|^p \text{ for a } p > 1 \text{ and } 0 < c_1 \leq c_2. \tag{3}$$

The inequality (2) describes the contraction between solutions through the point x and the point $x + v$. If the local contraction property (2) holds at all points of a positively invariant set, then the distance decreases for all solutions starting in this set, and for all positive times. This allows conclusions about the limit behaviour of all solutions within this set.

For more details on Finsler-Lyapunov functions and the relation to contraction analysis see [3]. In particular, (2) implies that the system is incrementally stable, i.e. the evolution of the distance between two adjacent solution is bounded for all positive times. If the inequality in (2) is replaced by sharper conditions, then the system can be shown to be incrementally asymptotically stable (distance converges to zero) or even incrementally exponentially stable (distance converges to zero exponentially fast).

While a Finsler-Lyapunov function satisfying (2) for all $v \in \mathbb{R}^n$ shows contraction in every direction v, we can modify the condition to capture only contraction in specific directions, e.g. to study problems with symmetry or to show the existence of periodic orbits as in this paper. To this end, a horizontal Finsler-Lyapunov function is defined in [3], where the tangent space at x is divided into a direct sum $\mathbb{R}^n = \mathcal{H}_x \bigoplus \mathcal{V}_x$ and (2) only is required for all $v \in \mathcal{H}_x$, i.e. the contraction is only guaranteed in horizontal direction.

Applied to periodic orbits, we choose $\mathcal{H}_x = \{v \in \mathbb{R}^n \mid v \perp f(x)\}$ and $\mathcal{V}_x = \text{span}(f(x))$ for all x which are no equilibria, and assume that (2) holds for all $v \in \mathcal{H}_x$. If $V(x, v)$ is a quadratic form in v, then [1, 11, 17] have shown under some additional assumptions that this implies the existence, uniqueness and stability of a periodic orbit and gives information about its basin of attraction. Further results using a contraction metric to establish existence, uniqueness, stability and information about the basin of attraction of a periodic orbit have been obtained in [10, 13].

[1] Note that Finsler-Lyapunov functions as defined in [3] are more general than considered in our case.

In this paper we numerically construct a Finsler-Lyapunov function by solving the PDE

$$\langle \nabla_x V(x,v), f(x)\rangle + (\nabla_v V(x,v))^T Df(x)v \quad = \quad -\|v\|^2 \tag{4}$$

using meshless collocation [19], which has been used to compute classical Lyapunov functions [5, 8]. One advantage of the proposed method is that the restrictions on the points v for which (4) is required, such as all v perpendicular to $f(x)$ for periodic orbits, can be easily implemented. We also require V to satisfy $V(x,0) = 0$ to obtain (3). This paper is an extended version of [7], where the method was first described.

We will also show that (4) has a solution for all x in the basin of attraction of an exponentially stable equilibrium or periodic orbit, which implies error estimates of the numerical method. Furthermore, we will explore the method near unstable equilibria. It turns out that we can still construct a function satisfying (4), but it no longer has the property (3). On the contrary, for the unstable directions $v \neq 0$ the function $V(x,v)$ is negative, while it is still positive for the stable ones. This can be used to detect the stable and unstable directions of equilibria.

Let us give an overview of the contents: In Section 2 we introduce meshless collocation in general and then apply it to our specific problem. Section 3 discusses existence results and error estimates for the cases of an equilibrium and periodic orbit. Section 4 presents the application of the method to three one- or two-dimensional with either an equilbrium or a periodic orbit. In Section 5 we discuss how the method can be used to detect the stability and stable/unstable directions of equilibria; we present three one- or two-dimensional examples to illustrate the method. We end with a discussion and conclusions in Section 6.

2 Meshless collocation

Meshless collocation, in particular by Radial Basis Functions, is used to interpolate multivariate functions and approximately solve Partial Differential Equations [15, 2, 16]. For a general introduction to meshless collocation and reproducing kernel Hilbert spaces (RKHS) see [19].

In this section we introduce meshless collocation. We first introduce Reproducing Kernel Hilbert Spaces, and then formulate the generalised interpolation problem, which in our case is a linear PDE with fixed function values. We follow [8, Section 2].

2.1 General method

We start with a short introduction to the general method of solving a generalized interpolation problem in a Reproducing Kernel Hilbert space of functions with domain in $\mathbb{R}^{2n}$, which is motivated by our application.

Let $O \subset \mathbb{R}^{2n}$ be a bounded set with Lipschitz continuous boundary. A Reproducing Kernel Hilbert Space (RKHS) is a Hilbert space H of functions $g\colon O \to \mathbb{R}$ with inner product $\langle \cdot, \cdot \rangle_H$ such that the following properties hold with a kernel $\Phi\colon O \times O \to \mathbb{R}$:

1. $\Phi(\cdot, \tilde{x}) \in H$ for all $\tilde{x} \in O$,

2. $g(\tilde{x}) = \langle g, \Phi(\cdot, \tilde{x}) \rangle_H$ for all $\tilde{x} \in O$ and $g \in H$.

We want to solve the following generalized interpolation problem:
Given $\tilde{N}$ linearly independent functionals $\lambda_1, \ldots, \lambda_{\tilde{N}} \in H^*$, where H^* denotes the dual of H, and $\tilde{N}$ numbers $\tilde{r}_i \in \mathbb{R}$, $i = 1, \ldots, \tilde{N}$, find the norm-minimal interpolant $s \in H$ satisfying

1. *$\lambda_i(s) = \tilde{r}_i$ for all $i = 1, \ldots, \tilde{N}$ (interpolant),*

2. *$\min\{\|s\|_H \mid s \in H, \lambda_i(s) = \tilde{r}_i$ for all $i = 1, \ldots, \tilde{N}\}$ (norm-minimal).*

It is well known that there is a unique norm-minimal interpolant, which is a linear combination of the Riesz representers of the functionals, and the coefficients can be determined by solving a system of $\tilde{N}$ linear equations. If H is a RKHS, then we have the following formula for the norm-minimal interpolant s:

$$s(\tilde{x}) \quad = \quad \sum_{j=1}^{\tilde{N}} \tilde{\alpha}_j \lambda_j^{\tilde{y}} \Phi(\tilde{x}, \tilde{y}), \tag{5}$$

where the superscript $\tilde{y}$ in $\lambda_j^{\tilde{y}}$ denotes the application of the functional with respect to $\tilde{y}$. Note that $\tilde{\alpha} \in \mathbb{R}^{\tilde{N}}$ is the solution of the linear system

$$\tilde{A}\tilde{\alpha} \quad = \quad \tilde{r}, \tag{6}$$

where $\tilde{r} = (\tilde{r}_i)_{i=1,\ldots,\tilde{N}} \in \mathbb{R}^{\tilde{N}}$ and $\tilde{A} = (\tilde{a}_{ij})_{i,j=1,\ldots,\tilde{N}} \in \mathbb{R}^{\tilde{N} \times \tilde{N}}$ is given by

$$\tilde{a}_{ij} \quad = \quad \lambda_i^{\tilde{x}} \lambda_j^{\tilde{y}} \Phi(\tilde{x}, \tilde{y}). \tag{7}$$

The matrix $\tilde{A}$ is positive definite, since the functionals are assumed to be linearly independent. In the following we consider the Sobolev space $W_2^\tau(\mathbb{R}^{2n})$ with $\tau > n$, which is a RKHS. While the reproducing kernel is rather complicated, there is a reproducing kernel, defined by a Wendland function, see Definition 2.1, which generates the same Hilbert space, but with a different, yet equivalent norm.

Definition 2.1 (see [18]) *Let $k \in \mathbb{N}_0$ and $l \in \mathbb{N}$. We denote $x_+ = x$ for $x \geq 0$ and $x_+ = 0$ for $x < 0$. We define the Wendland functions $\psi_{l,k}$ for $r \in \mathbb{R}_0^+$ by recursion*

$$\psi_{l,0}(r) = (1 - r)_+^l, \qquad \psi_{l,k+1}(r) = \int_r^1 t\psi_{l,k}(t)\, dt.$$

The following proposition follows from [8, Proposition 3.11] and the arguments in the proof; note that the space dimension in our case is $2n$.

Proposition 2.2 *Let $k \in \mathbb{N}$, $c \in \mathbb{R}^+$ and set $l = n + k + 1$. Define $\psi_0(r) = \psi_{l,k}(cr)$, where $\psi_{l,k}$ was defined in Definition 2.1, and $\Phi(\tilde{x}, \tilde{y}) = \psi_0(\|\tilde{x} - \tilde{y}\|)$, where $\|\cdot\|$ denotes the Euclidean norm in $\mathbb{R}^{2n}$. Then $\Phi \in C^{2k}$ is a reproducing kernel of $W_2^\tau(\mathbb{R}^{2n})$ with $\tau = k + n + \frac{1}{2}$ (and equivalent norm).*

From now on, we choose a Wendland function with smoothness degree $k \geq 2$ and choose Φ to be the kernel of the RKHS $H = W_2^\tau(\mathbb{R}^{2n})$ as above with $\tau = k + n + \frac{1}{2}$.

Now let us apply this method to solve the problem

$$LV(\tilde{x}) = r(\tilde{x}) \text{ for } \tilde{x} \in O, \tag{8}$$

$$V(\tilde{x}) = r_0(\tilde{x}) \text{ for } \tilde{x} \in \Gamma, \tag{9}$$

where L is a first-order differential operator of the form

$$LV(\tilde{x}) = \sum_{|\beta| \leq 1} c_\beta(\tilde{x}) D^\beta V(\tilde{x}), \tag{10}$$

$c_\beta \colon O \to \mathbb{R}$, $r(\tilde{x})$ and $r_0(\tilde{x})$ are given functions and $O, \Gamma \subset \mathbb{R}^{2n}$. We call a point $\tilde{x} \in \mathbb{R}^{2n}$ a singular point of L if $c_\beta(\tilde{x}) = 0$ for all $|\beta| \leq 1$, see [8, Definition 3.2].

We choose collocation points $X_1 = \{\tilde{x}_1, \ldots, \tilde{x}_N\} \subset O$ and $X_2 = \{\tilde{\xi}_1, \ldots, \tilde{\xi}_M\} \subset \Gamma$ and define the functionals $\lambda_j = \delta_{\tilde{x}_j} \circ L$, $j = 1, \ldots, N$ and $\lambda_{N+j} = \delta_{\tilde{\xi}_j} \circ \mathrm{id}$, $j = 1, \ldots, M$. These $\tilde{N} = N + M$ functionals are linearly independent if the collocation points x_j are no singular points of L, see [8, Proposition 3.3]; note that $\tau > 1 + n$.

We then have error estimates in terms of the mesh-norms $h_{X_1,O} = \sup_{\tilde{x} \in O} \min_{\tilde{x}_j \in X_1} \|\tilde{x} - \tilde{x}_j\|$ and $h_{X_2,\Gamma} = \sup_{\tilde{y} \in \Gamma} \min_{\tilde{\xi}_j \in X_2} \|\tilde{y} - \tilde{\xi}_j\|$, which measure how dense the collocation points X_1 lie in O and X_2 in Γ, respectively. Note that the error estimates in [8, Corollary 3.12] hold in the same way if Γ is not part of the boundary of O, but a smooth, $(n-1)$-dimensional subset of O.

Theorem 2.3 *Let Γ be a smooth, $(n-1)$-dimensional subset of $O \subset \mathbb{R}^n$, where O is a bounded domain with Lipschitz continuous boundary. Let $c_\beta \in W_\infty^{k+n}(O)$ and let the solution V of (8) and (9) satisfy $V \in W_2^{k+n+1/2}(O)$. Let $X_1 = \{\tilde{x}_1, \ldots, \tilde{x}_N\} \subset O$ be pairwise distinct points, which are not singular points of L, and $X_2 = \{\tilde{\xi}_1, \ldots, \tilde{\xi}_M\} \subset \Gamma$ be pairwise distinct points. We denote by s the norm-minimal interpolant of the data.*

Then, for sufficiently small mesh-norms, we have

$$\|LV - Ls\|_{L_\infty(O)} \leq C h_{X_1,O}^{k-1/2} \|V\|_{W_2^{k+n+1/2}(O)}, \tag{11}$$

$$\|V - s\|_{L_\infty(\Gamma)} \leq C h_{X_2,\Gamma}^{k+1/2} \|V\|_{W_2^{k+n+1/2}(O)}, \tag{12}$$

where C is a constant independent of V.

2.2 Application to our specific problem

We denote $\tilde{x} = (x, v) \in \mathbb{R}^{2n}$. We define the differential operator L acting on a function $V(x, v)$, where $x, v \in \mathbb{R}^n$ by

$$LV(x, v) = \langle \nabla_x V(x, v), f(x) \rangle + (\nabla_v V(x, v))^T Df(x) v. \tag{13}$$

We wish to solve the problem

$$\left\{ \begin{array}{lcl} LV(x,v) & = & -\|v\|^2, \\ V(x,0) & = & 0. \end{array} \right. \tag{14}$$

Note that the first equation in (14) is (4). The second equation in (14) fixes the values of $V(x,0) = 0$ at $v = 0$, since otherwise the function V will in general not satisfy (3).

Lemma 2.4 *$(x,v) \in \mathbb{R}^{2n}$ is a singular point of L as defined in* (13) *if and only if $f(x) = 0$ (x is equilibrium) and $Df(x)v = 0$.*

PROOF: L is a first-order differential operator of the form (10) with $c_{e_i}(x,v) = f_i(x)$ for $i = 1,\ldots,n$ and $c_{e_i}(x,v) = (Df(x)v)_{i-n}$ for $i = n+1,\ldots,2n$. A singular point is a point (x,v) such that all $c_{e_i}(x,v) = 0$. □

We fix a bounded set $K \subset \mathbb{R}^n$ with Lipschitz continuous boundary and define $B_r(0) := \{v \in \mathbb{R}^n \mid \|v\| \leq r\}$ with $r > 0$ small. We choose points $\tilde{x}_j \in K \times B_r(0)$ for $j = 1,\ldots,N$, which are no singular points of L, see Lemma 2.4, and denote this set of points by $X_1 := \{\tilde{x}_1, \tilde{x}_2, \ldots, \tilde{x}_N\}$. Moreover, we choose points for which we fix the values of $V(x,0)$, namely $\tilde{\xi}_j = (\xi_j, 0) \in K \times \{0\} =: \Gamma$ for $j = 1,\ldots,M$; we denote this set of points by $X_2 := \{\tilde{\xi}_1, \ldots, \tilde{\xi}_M\}$.

The norm-minimal interpolant v of the function V with the data above is given by (5), namely

$$s(\tilde{x}) \quad = \quad \sum_{k=1}^{N} \alpha_k (\delta_{\tilde{x}_k} \circ L)^{\tilde{y}} \psi_0(\|\tilde{x} - \tilde{y}\|) + \sum_{k=1}^{M} \beta_k \psi_0(\|\tilde{x} - \tilde{\xi}_k\|), \tag{15}$$

where ψ_0 was defined in Proposition 2.2. The coefficient vector is the solution of the following system of linear equations, see (6),

$$\widetilde{A} \left(\begin{array}{c} \alpha \\ \beta \end{array} \right) = \left(\begin{array}{c} a \\ b \end{array} \right) \text{ with } \widetilde{A} := \left(\begin{array}{cc} A & D \\ D^T & B \end{array} \right) \in \mathbb{R}^{(N+M)\times(N+M)}. \tag{16}$$

The right-hand side of the linear system (16) is determined by $a_j = -\|v_j\|^2$ for $1 \leq j \leq N$ and $b_j = 0$ for $1 \leq j \leq M$. The sub-matrices $A = (a_{jk}) \in \mathbb{R}^{N\times N}$, $B = (b_{jk}) \in \mathbb{R}^{M\times M}$ and $D = (d_{jk}) \in \mathbb{R}^{N\times M}$ have the elements, see (7),

$$\begin{array}{lcl} a_{jk} & = & (\delta_{\tilde{x}_j} \circ L)^{\tilde{x}} (\delta_{\tilde{x}_k} \circ L)^{\tilde{y}} \psi_0(\|\tilde{x} - \tilde{y}\|), \\ b_{jk} & = & \psi_0(\|\tilde{\xi}_j - \tilde{\xi}_k\|), \\ d_{jk} & = & (\delta_{\tilde{x}_j} \circ L)^{\tilde{x}} \psi_0(\|\tilde{x} - \tilde{\xi}_k\|). \end{array}$$

To compute d_{jk} and a_{jk} explicitly, let us recursively define $\psi_{i+1}(r) = \frac{1}{r}\frac{\partial \psi_i(r)}{\partial r}$ for $i = 0, 1$ and $r > 0$. Note that for the Wendland functions with smoothness parameter $k \geq 2$ these functions can be continued continuously up to $r = 0$.

We have, denoting $\tilde{x} = (x, v)$, $\tilde{y} = (y, w)$, $\tilde{x}_j = (x_j, v_j)$ and $\tilde{\xi}_k = (\xi_k, \eta_k)$

$$d_{jk} = \psi_1(\|\tilde{x}_j - \tilde{\xi}_k\|)\left[\langle x_j - \xi_k, f(x_j)\rangle + (v_j - \eta_k)^T Df(x_j)v_j\right].$$

Using the notation $x_{jk} = x_j - x_k$ and $v_{jk} = v_j - v_k$ we have

$$\begin{aligned} a_{jk} &= -\psi_2(\|\tilde{x}_j - \tilde{x}_k\|)\big[\langle x_{jk}, f(x_k)\rangle\langle x_{jk}, f(x_j)\rangle + v_{jk}^T Df(x_k)v_k\langle x_{jk}, f(x_j)\rangle \\ &\qquad + \langle x_{jk}, f(x_k)\rangle v_{jk}^T Df(x_j)v_j + v_{jk}^T Df(x_k)v_k \cdot v_{jk}^T Df(x_j)v_j\big] \\ &\quad -\psi_1(\|\tilde{x}_j - \tilde{x}_k\|)\left[\langle f(x_k), f(x_j)\rangle + v_k^T Df(x_k)^T Df(x_j)v_j\right]. \end{aligned}$$

We have, similarly to the computation of a_{jk} the following formula, using the notation $x_{\cdot k} = x - x_k$ and $v_{\cdot k} = v - v_k$, see (15)

$$\begin{aligned} Ls(x,v) &= \sum_{k=1}^N \alpha_k(\delta_{\tilde{x}} \circ L)^{\tilde{x}}(\delta_{\tilde{x}_l} \circ L)^{\tilde{y}}\psi_0(\|\tilde{x} - \tilde{y}\|) + \sum_{k=1}^M \beta_k(\delta_{\tilde{x}} \circ L)^{\tilde{x}}\psi_0(\|\tilde{x} - \tilde{\xi}_k\|) \\ &= -\sum_{k=1}^N \alpha_k\Big\{\psi_2(\|\tilde{x} - \tilde{x}_k\|)\big[\langle x_{\cdot k}, f(x_k)\rangle\langle x_{\cdot k}, f(x)\rangle + v_{\cdot k}^T Df(x_k)v_k\langle x_{\cdot k}, f(x)\rangle \\ &\qquad + \langle x_{\cdot k}, f(x_k)\rangle v_{\cdot k}^T Df(x)v + v_{\cdot k}^T Df(x_k)v_k \cdot v_{\cdot k}^T Df(x)v\big] \\ &\qquad + \psi_1(\|\tilde{x} - \tilde{x}_k\|)\left[\langle f(x_k), f(x)\rangle + v_k^T Df(x_k)^T Df(x)v\right]\Big\} \\ &\quad + \sum_{k=1}^M \beta_k\psi_1(\|\tilde{x} - \tilde{\xi}_k\|)\left[\langle x - \xi_k, f(x)\rangle + (v - \eta_k)^T Df(x)v\right]. \end{aligned}$$

3 Existence and error estimates

In certain dynamical situations we can prove the existence of a function satisfying (14), enabling us to obtain error estimates. In Proposition 3.1 we consider an exponentially stable equilibrium and in Proposition 3.2 an exponentially stable periodic orbit – in each case we show that a function V satisfying (14) exists for all x in its basin of attraction. Hence, we can use the error estimates, see Proposition 3.3, comparing the approximation to the existing solution of the problem.

Proposition 3.1 *Assume that x_0 is an exponentially stable equilibrium of (1), where $f \in C^\sigma(\mathbb{R}^n, \mathbb{R}^n)$, $\sigma \geq 2$, with basin of attraction $A(x_0)$.*

Then there is a function $V \in C^{\sigma-1}(A(x_0) \times \mathbb{R}^n, \mathbb{R})$ satisfying (14) for all $(x, v) \in A(x_0) \times \mathbb{R}^n$. For any compact set $K \subset A(x_0)$ there are constants $c_1, c_2 > 0$ such that $c_1\|v\|^2 \leq V(x, v) \leq c_2\|v\|^2$ holds for all $x \in K$.

PROOF: Choose the positive definite matrix $C = I \in \mathbb{S}^n$, where $\mathbb{S}^n$ denotes the symmetric matrices in $\mathbb{R}^{n\times n}$. By [6, Theorem 4.4] there exists a matrix-valued function $M \in C^{\sigma-1}(A(x_0), \mathbb{S}^n)$, such that $M(x)$ is positive definite for all $x \in A(x_0)$, satisfying

$$Df(x)^T M(x) + M(x)Df(x) + \dot{M}(x) = -I \text{ for all } x \in A(x_0). \tag{17}$$

Here, $\dot{M}(x)$ denotes the matrix with entries $\langle \nabla_x M_{ij}(x), f(x)\rangle$, $i,j = 1,\dots,n$, the orbital derivative of $M(x)$. Define $V \in C^{\sigma-1}(A(x_0)\times\mathbb{R}^n,\mathbb{R})$ by $V(x,v) = v^T M(x) v$. The positive definiteness of M implies the estimate on $V(x,v)$ in a compact set. We have $V(x,0) = 0$ for all $x \in A(x_0)$ and

$$\begin{aligned} LV(x,v) &= \langle \nabla_x V(x,v), f(x)\rangle + (\nabla_v V(x,v))^T Df(x)v \\ &= v^T \dot{M}(x)v + v^T M(x) Df(x)v + v^T Df(x)^T M(x)v \\ &= -\|v\|^2 \text{ by (17)} \end{aligned}$$

for all $x \in A(x_0)$ and $v \in \mathbb{R}^n$. □

For a periodic orbit, we have the following result.

Proposition 3.2 *Assume that Ω is an exponentially stable periodic orbit of (1), where $f \in C^\sigma(\mathbb{R}^n,\mathbb{R}^n)$, $\sigma \geq 2$, with basin of attraction $A(\Omega)$.*

Then there is a function $V \in C^{\sigma-1}(A(\Omega),\mathbb{R}^n)$ satisfying

$$LV(x,v) = -\|v\|^2 \tag{18}$$

for all $v \perp f(x)$. For any compact set $K \subset A(\Omega)$ there are constants $c_1, c_2 > 0$ such that

$$c_1\|v\|^2 \leq V(x,v) \leq c_2\|v\|^2 \tag{19}$$

holds for all $x \in K$ and $v \perp f(x)$.

Proof: Define

$$P_x = I - \frac{f(x)f(x)^T}{\|f(x)\|^2},$$

which is a projection onto the hyperplane perpendicular to $f(x)$, i.e. $f(x)^T P_x v = 0$ for all $v \in \mathbb{R}^n$, $P_x f(x) = 0$, $P_x v = v$ for all $v \in \mathbb{R}^n$ with $v^T f(x) = 0$ and $P_x P_x = P_x$. Note that

$$\begin{aligned} \dot{P}_x &= -\frac{Df(x)f(x)f(x)^T + f(x)f(x)^T Df(x)^T}{\|f(x)\|^2} \\ &\quad + \frac{f(x)f(x)^T f(x)^T [Df(x) + Df(x)^T] f(x)}{\|f(x)\|^4}. \end{aligned} \tag{20}$$

Let $B \in \mathbb{S}^n$ be a positive definite matrix. By [4, Theorem 3.1] there exists a matrix-valued function $M \in C^{\sigma-1}(A(\Omega),\mathbb{S}^n)$ such that $M(x)$ is positive definite for all $x \in A(\Omega)$ and it satisfies

$$LM(x) = -P_x B P_x \text{ for all } x \in A(\Omega), \tag{21}$$

$$\begin{aligned} \text{where } LM(x) &= Df(x)^T M(x) + M(x)Df(x) + \dot{M}(x) \\ &\quad - \frac{M(x)f(x)f(x)^T (Df(x) + Df(x)^T)}{\|f(x)\|^2} \\ &\quad - \frac{(Df(x) + Df(x)^T) f(x)f(x)^T M(x)}{\|f(x)\|^2}. \end{aligned} \tag{22}$$

Here, $\dot{M}(x)$ denotes the matrix with entries $\langle \nabla_x M_{ij}(x), f(x)\rangle$, $i,j = 1,\dots,n$, the orbital derivative of $M(x)$.

We define the function $V \in C^{\sigma-1}(A(x_0)\times\mathbb{R}^n,\mathbb{R})$ by

$$V(x,v) = v^T P_x M(x) P_x v.$$

We have $V(x,0) = 0$ for all $x \in A(\Omega)$. For all $v \in \mathbb{R}^n$ with $v^T f(x) = 0$ we have

$$V(x,v) = v^T M(x) v.$$

Denoting by $\Lambda(x)$ the largest and by $\lambda(x)$ the smallest eigenvalue of the positive definite matrix $M(x)$, we define for a compact set $K \subset A(\Omega)$ the positive constants $c_1 = \min_{x\in K}\lambda(x)$ and $c_2 = \max_{x\in K}\Lambda(x)$, which shows (19). Moreover, we have,

$$\begin{aligned} LV(x,v) &= \langle \nabla_x V(x,v), f(x)\rangle + (\nabla_v V(x,v))^T Df(x)v \\ &= v^T[\dot{P}_x M(x)P_x + P_x\dot{M}(x)P_x + P_x M(x)\dot{P}_x \\ &\quad + Df(x)^T P_x M(x)P_x + P_x M(x)P_x Df(x)]v\,. \end{aligned}$$

We have, using (20)

$$
\begin{aligned}
&\dot{P}_x M(x) P_x + P_x \dot{M}(x) P_x + P_x M(x) \dot{P}_x + Df(x)^T P_x M(x) P_x + P_x M(x) P_x Df(x) \\
= \; & -\frac{Df(x)f(x)f(x)^T + f(x)f(x)^T Df(x)^T}{\|f(x)\|^2} M(x) P_x \\
& + \frac{f(x)f(x)^T f(x)^T [Df(x) + Df(x)^T] f(x)}{\|f(x)\|^4} M(x) P_x \\
& + P_x \dot{M}(x) P_x \\
& - P_x M(x) \frac{Df(x)f(x)f(x)^T + f(x)f(x)^T Df(x)^T}{\|f(x)\|^2} \\
& + P_x M(x) \frac{f(x)f(x)^T f(x)^T [Df(x) + Df(x)^T] f(x)}{\|f(x)\|^4} \\
& + Df(x)^T \left(I - \frac{f(x)f(x)^T}{\|f(x)\|^2} \right) M(x) P_x \\
& + P_x M(x) \left(I - \frac{f(x)f(x)^T}{\|f(x)\|^2} \right) Df(x) \\
= \; & \left(I - \frac{f(x)f(x)^T}{\|f(x)\|^2} \right) \Bigg[Df(x)^T M(x) + M(x) Df(x) + \dot{M}(x) \\
& - \frac{M(x)f(x)f(x)^T (Df(x) + Df(x)^T)}{\|f(x)\|^2} \\
& - \frac{(Df(x) + Df(x)^T) f(x) f(x)^T M(x)}{\|f(x)\|^2} \Bigg] \left(I - \frac{f(x)f(x)^T}{\|f(x)\|^2} \right) \\
= \; & P_x \Bigg[Df(x)^T M(x) + M(x) Df(x) + \dot{M}(x) \\
& - \frac{M(x)f(x)f(x)^T (Df(x) + Df(x)^T)}{\|f(x)\|^2} \\
& - \frac{(Df(x) + Df(x)^T) f(x) f(x)^T M(x)}{\|f(x)\|^2} \Bigg] P_x \\
= \; & -P_x P_x B P_x P_x \text{ by (21)} \\
= \; & -P_x B P_x \, .
\end{aligned}
$$

Hence, for all $x \in A(x_0)$ and $v \in \mathbb{R}^n$ with $v^T f(x) = 0$ we have

$$
\begin{aligned}
LV(x,v) &= -v^T P_x B P_x v \\
&= -v^T B v,
\end{aligned}
$$

which proves (18) when choosing $B = I$. □

In the situations as above, where we know that a solution V with a certain smoothness exists, we can use the error estimate Theorem 2.3.

Proposition 3.3 *Let $k \geq 2$ be the smoothness degree of the Wendland function. In the situation of Proposition 3.1 or 3.2 let $f \in C^\sigma(\mathbb{R}^n, \mathbb{R}^n)$ with $\sigma \geq k + n + 3/2$, $B \subset \overline{B} \subset A(x_0)$, $A(\Omega)$, respectively be an open bounded set with Lipschitz continuous boundary and $\Gamma = \{(x, 0) \mid x \in B\}$.*

Then, for the collocation points as described in Theorem 2.3 the estimates (11) *and* (12) *hold.*

PROOF: Let $O = B \times B_R(0)$ with $R > 0$. We check that the assumptions of Theorem 2.3 are satisfied: we have $c_\beta \in C^{\sigma-1}(\mathbb{R}^n) \subset W_\infty^{k+n}(O)$ and by Proposition 3.1 or 3.2 we have for the solution $V \in C^{\sigma-1}(A(x_0) \times \mathbb{R}^n, \mathbb{R}) \subset W_2^{k+n+1/2}(O)$, $V \in C^{\sigma-1}(A(\Omega) \times \mathbb{R}^n, \mathbb{R}) \subset W_2^{k+n+1/2}(O)$, respectively. □

4 Examples

4.1 One-dimensional example

We consider $n = 1$ and the dynamical system given by

$$\dot{x} \quad = \quad x - x^3 \tag{23}$$

which has one asymptotically stable equilibrium at 0 and two unstable equilibria at ± 1. We use the Wendland function $\psi_0(r) = \psi_{4,2}(r) = (1-r)_+^6(35r^2 + 18r + 3)$ and the collocation points $X_1 = (\rho\mathbb{Z} \cap [-0.7, 0.7]) \times (\tau\mathbb{Z} \cap [-0.1, 0.1]) \setminus \{(0, 0)\}$ with $\rho = \frac{0.7}{19} = 0.0368$ and $\tau = \frac{0.1}{3} = 0.0333$; note that $(0, 0)$ is a singular point of L. Furthermore, we choose $X_2 = (\rho\mathbb{Z} \cap [-0.7, 0.7]) \times \{0\}$. The grids have $N = 272$ and $M = 39$ points, respectively, so together $\tilde{N} = N + M = 311$.

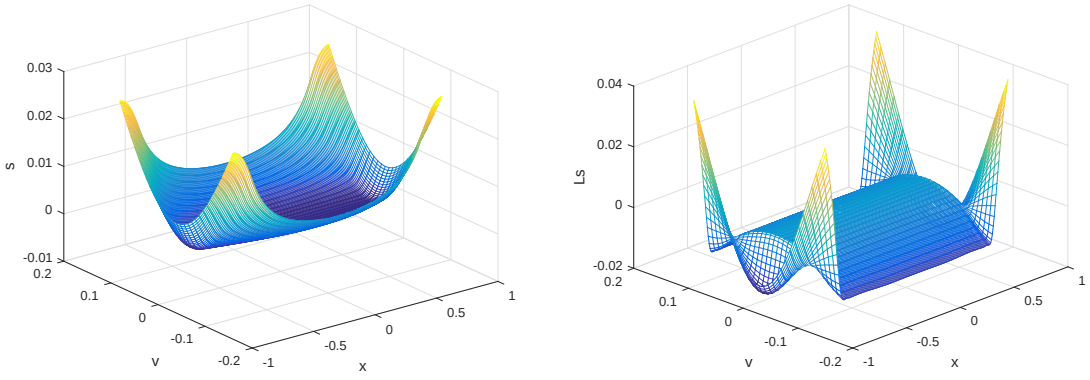

Figure 1: Example (23). Left: The function $s(x, v)$. Right: The function $Ls(x, v)$ which approximates $-\|v\|^2$ well.

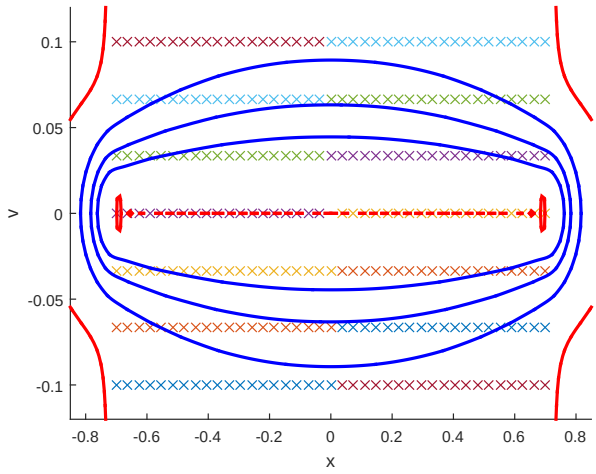

Figure 2: Example (23): The collocation points as well as the level sets $Ls(x,v) = 0$ (red) and $s(x,v) = 0, 0.005, 0.01$ (blue). Note that $Ls(x,v) < 0$ holds in the area where the collocation points are placed, apart from a small area near $v = 0$.

Figure 1, left, shows the computed function $s(x,v)$, which satisfies $c_1\|v\|^2 \le s(x,v) \le c_2\|v\|^2$, as well as $Ls(x,v)$ which approximates $-\|v\|^2$ well. Figure 2 shows the collocation points, the area where $Ls(x,v) = 0$ (red) as well as some level sets of $s(x,v)$ (blue) in the area where $s(x,v)$ satisfies the conditions.

4.2 Two-dimensional example – stable equilibrium

We consider $n = 2$ and the dynamical system given by

$$\left\{ \begin{array}{rcl} \dot{x} &=& -x(1-x^2-y^2)+y \\ \dot{y} &=& -y(1-x^2-y^2)-x \end{array} \right. \tag{24}$$

which has an asymptotically stable equilibrium at the origin and an unstable periodic orbit at the unit circle. We denote $\mathbf{x} = (x,y) \in \mathbb{R}^2$ and $\mathbf{v} = (v,w) \in \mathbb{R}^2$.

We use the Wendland function $\psi_{5,2}(r) = (1-r)_+^7(16r^2+7r+1)$ and the collocation points defined below containing $N = 8580$ and $M = 441$ points, respectively; altogether we have $\tilde{N} = N + M = 9021$ points.

$$\begin{array}{rcl} X_1 &=& \big\{(\mathbf{x},\mathbf{v}) \in B_{0.9}(0,0) \times \mathbb{R}^2 \mid x,y \in 0.07 \cdot \mathbb{Z} \cap [-0.7,0.7], \\ && \qquad \mathbf{v} \in \{r(\cos(\theta),\sin(\theta)), r \in \{0.05,0.1\}, \theta = 2k\pi/10, k = 1,\dots,10\}\big\}, \text{ and} \\ X_2 &=& \{(\mathbf{x},0) \in \mathbb{R}^2 \times \mathbb{R}^2 \mid x,y \in 0.07 \cdot \mathbb{Z} \cap [-0.7,0.7]\}. \end{array}$$

Figure 3 shows points $\mathbf{x}$ where $Ls(\mathbf{x},\mathbf{v})$ was evaluated for many $\mathbf{v} \neq 0$. For each $\mathbf{v}$ where $Ls(\mathbf{x},\mathbf{v}) < 0$, a blue circle was plotted at the position $\mathbf{x}$, while for each $\mathbf{v}$ where $Ls(\mathbf{x},\mathbf{v}) \ge 0$ a red cross was drawn at position $\mathbf{x}$. Points $\mathbf{x}$ can thus have both a blue circle and a red cross, meaning that some directions $\mathbf{v}$ have the correct (negative) sign, while

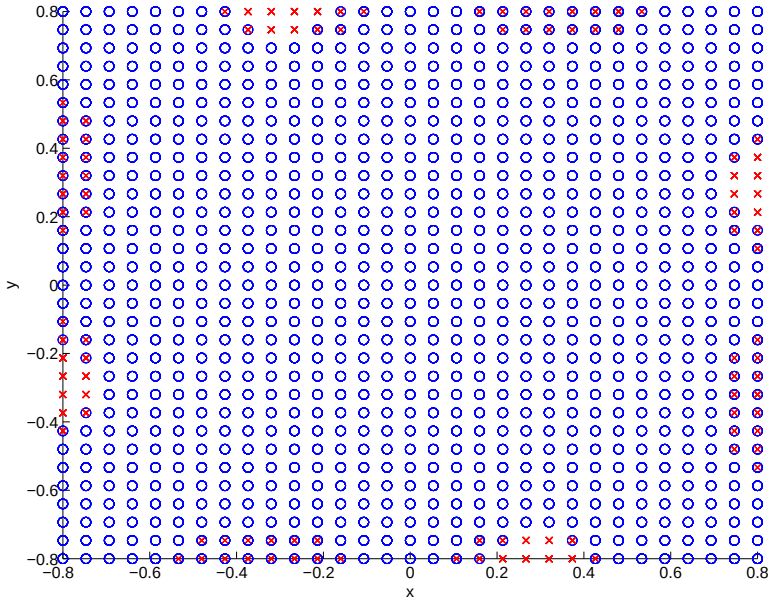

Figure 3: Example (24): Some points in the $\mathbf{x} = (x, y)$-plane, where the sign of $L(\mathbf{x}, \mathbf{v})$ is calculated: if the sign of $L(\mathbf{x}, \mathbf{v})$ is negative for a $\mathbf{v}$, then a blue circle is plotted, if the sign is non-positive for a $\mathbf{v}$, then a red cross is plotted. The points with the correct, negative sign are thus points with a blue circle only.

others have not. Points with only a blue circle are points where Ls has the correct sign, while points with any red cross are not. One can clearly see that the square $[-0.7, 0.7]^2$, where the collocation points where placed, contains only blue circles.

Figure 4 shows the functions $s(\mathbf{x}_0, \mathbf{v})$ and $Ls(\mathbf{x}_0, \mathbf{v})$ for a fixed $\mathbf{x}_0 = (0.5, 0.5)$; note that no point $(\mathbf{x}_0, \mathbf{v})$ is a collocation point. The function $Ls(\mathbf{x}_0, \mathbf{v})$ approximates $-\|\mathbf{v}\|^2$ well (left) and the function $s(\mathbf{x}_0, \mathbf{v})$, right, satisfies $c_1\|\mathbf{v}\|^2 \leq s(\mathbf{x}_0, \mathbf{v}) \leq c_2\|\mathbf{v}\|^2$.

4.3 Two-dimensional example – stable periodic orbit

We consider the dynamical system given by

$$\begin{cases} \dot{x} &= x(1 - x^2 - y^2) + y \\ \dot{y} &= y(1 - x^2 - y^2) - x \end{cases} \tag{25}$$

which has an unstable equilibrium at the origin and an asymptotically stable periodic orbit at the unit circle. This time we solve the problem

$$\begin{cases} LV(x, v) &= -\|v\|^2 \text{ for } v \perp f(x) \\ V(x, 0) &= 0. \end{cases} \tag{26}$$

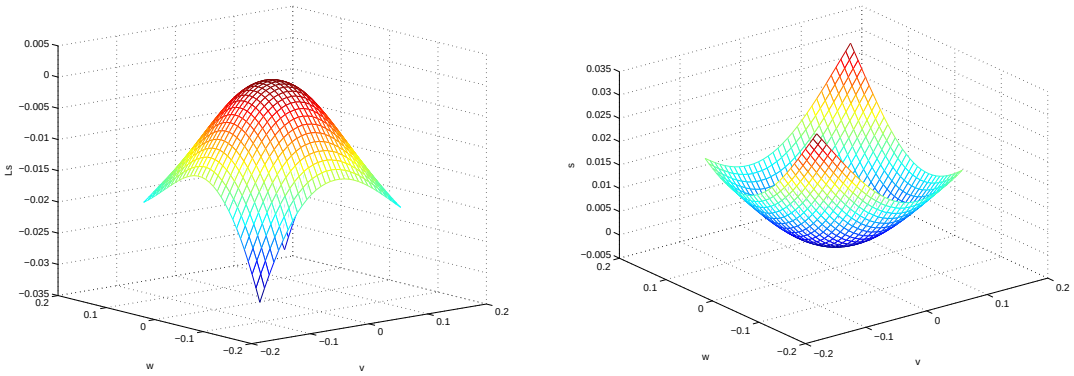

Figure 4: Example (24). Left: The function $Ls((0.5, 0.5), (v, w))$ which approximates $-\|(v, w)\|^2$ well. Right: The function $s((0.5, 0.5), (v, w))$ which has its minimum 0 at $(v, w) = (0, 0)$. Note that no $(\mathbf{x}_0, \mathbf{v})$ with $\mathbf{x}_0 = (0.5, 0.5)$ is a collocation point.

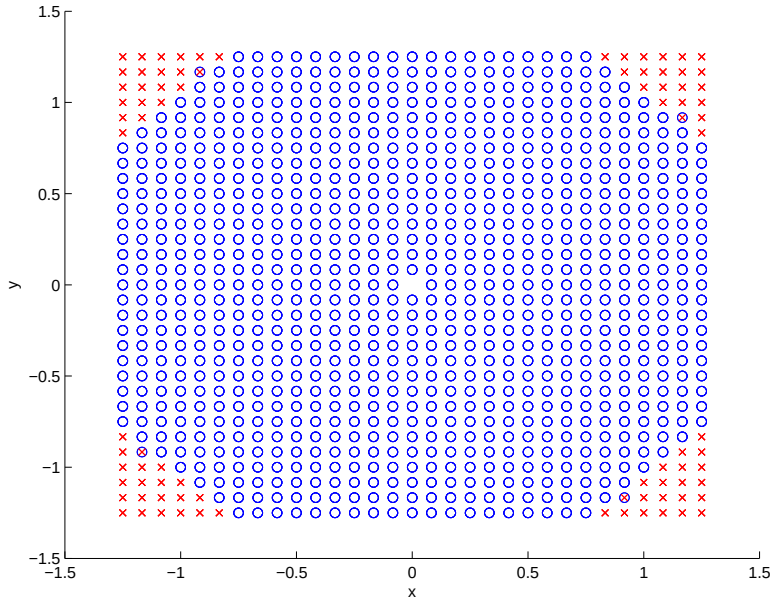

Figure 5: Example (25): Some points in the $\mathbf{x} = (x, y)$-plane, where the sign of $Ls(\mathbf{x}, \mathbf{v})$ is calculated: if the sign of $Ls(\mathbf{x}, \mathbf{v})$ is negative for all directions $\mathbf{v} \perp f(\mathbf{x})$, then a blue circle is plotted, if the sign is non-positive for all directions $\mathbf{v} \perp f(\mathbf{x})$, then a red cross is plotted, and if some directions $\mathbf{v}$ result in a negative and some in a non-negative sign, then both a red cross and a blue circle are plotted. The points with the correct, negative sign are thus points with a blue circle.

We use the Wendland function $\psi_{5,2}(r) = (1-r)_+^7(16r^2+7r+1)$ and the points

$$\begin{aligned} X_1 &= \big\{(\mathbf{x},\mathbf{v}) \in (B_{1.3}(0,0) \setminus \{(0,0)\}) \times \mathbb{R}^2 \mid x, y \in \rho\,\mathbb{Z} \cap [-1.2, 1.2], \\ &\qquad \mathbf{v} \in \{\pm 0.05\, f(\mathbf{x})/\|f(\mathbf{x})\|, \pm 0.1\, f(\mathbf{x})/\|f(\mathbf{x})\|\}\big\} \\ X_2 &= \{(\mathbf{x},0) \in B_{1.3}(0,0) \times \mathbb{R}^2 \mid x, y \in \rho\,\mathbb{Z} \cap [-1.2, 1.2]\}, \end{aligned}$$

where $\rho = \frac{1.2}{9} = 0.1333$, with $N = 1168$ and $M = 293$ points, respectively, altogether $\tilde{N} = N + M = 1461$ points.

Figure 5 shows points $\mathbf{x}$ where $Ls(\mathbf{x},\mathbf{v})$ was evaluated for several $\mathbf{v} \perp f(\mathbf{x})$. For each $\mathbf{v}$ where $Ls(\mathbf{x},\mathbf{v}) < 0$, a blue circle was added, while for each $\mathbf{v}$ where $Ls(\mathbf{x},\mathbf{v}) \geq 0$ a red cross was drawn. Points with only a blue circle are points where Ls has the correct (negative) sign, while points with any red cross are not. One can clearly see that the ball of radius 1.3, where the collocation points where placed, contains only blue circles.

5 Detecting stable and unstable directions

In this section we explore how the numerical procedure can be used to detect and analyse other dynamical situations. In particular, we consider the case of an unstable equilibrium. A function satisfying (14) may still exist near an unstable equilibrium, but it will not satisfy $c_1\|V\|^p \leq V(x,v) \leq c_2\|V\|^p$ for all $v \in \mathbb{R}^n$, which we will call positive definite in this context. For unstable equilibria with an n-dimensional unstable manifold, we will have $-c_1\|v\|^p \leq V(x,v) \leq -c_2\|v\|^p$, while for saddle points we will have $V(x,v) > 0$ for the stable directions v and $V(x,v) < 0$ for the unstable directions v.

5.1 One-dimensional case

Before we consider examples, let us compute V in general. We make the ansatz $V(x,v) = v^T M(x) v$, which satisfies $V(x,0) = 0$. Note that in the 1-dimensional case this results in $V(x,v) = m(x)v^2$.

For a general system (1) we have with this ansatz

$$LV(x,v) = v^T[\dot{M}(x) + Df(x)^T M(x) + M(x)Df(x)]v.$$

To achieve $LV(x,v) = -\|v\|^2$ we require

$$\dot{M}(x) + Df(x)^T M(x) + M(x)Df(x) = -I. \tag{27}$$

In the 1-dimensional case, we thus need to solve, setting $M(x) = m(x) \in \mathbb{R}$

$$m'(x)f(x) + 2m(x)f'(x) = -1.$$

The solution of this inhomogeneous linear differential equation is

$$m(x) = \frac{-F(x) + C}{f(x)^2},$$

where F is a primitive function of f. The function $m(x)$ is not defined at equilibria in general, however, by choosing the integration constant C appropriately, it may be defined at certain equilibria.

Now let us consider the example with $f(x) = x(1-x^2)$, i.e.

$$\dot{x} \;=\; x(1-x^2) \tag{28}$$

which has two asymptotically stable equilibria at ± 1 and one unstable equilibrium at 0. Following the procedure described above, we have $F(x) = \frac{1}{2}x^2 - \frac{1}{4}x^4$ and

$$m(x) \;=\; \frac{1}{4}\frac{x^4 - 2x^2 + 4C}{x^2(1-x^2)^2}\,.$$

For $m(x)$ to be defined at the asymptotically stable equilibria $x = \pm 1$, choose $C = \frac{1}{4}$ and then we obtain

$$m(x) \;=\; \frac{1}{4x^2},$$

which is defined in $\mathbb{R}\backslash\{0\}$. Note that here $V(x,v) = \frac{v^2}{4x^2}$ is positive definite, i.e. $V(x,v) > 0$ for all $v \neq 0$ and $x \in \mathbb{R} \setminus \{0\}$, and thus is a Finsler-Lyapunov function as before.

However, by choosing the constant $C = 0$, $m(x)$ can also be defined at the unstable equilibrium $x = 0$. Indeed, we obtain

$$m(x) \;=\; \frac{1}{4}\frac{x^2 - 2}{(1-x^2)^2},$$

which is defined in $(-1,1)$, but $m(x) < 0$; hence $V(x,v) = \frac{1}{4}\frac{x^2-2}{(1-x^2)^2}v^2$ is negative definite, i.e. $V(x,v) < 0$ for all $v \neq 0$ and $x \in (-1,1)$.

If we place the collocation points away from the respective singular set, then we approximate either of the two functions and thus obtain the result above. For all calculations in this section we have used the Wendland function $\psi_0(r) = \psi_{4,2}(r) = (1-r)_+^6(35r^2+18r+3)$.

First, we do not set any collocation points near the unstable equilibrium at 0 and obtain a Finsler-Lyapunov function. In detail, we choose the collocation points

$$\begin{aligned} X_1 \;&=\; \left\{(x,v) \in \left(\frac{1}{30}\mathbb{Z} \cap [-2.5, 2.5] \setminus [-0.2, 0.2]\right) \times \left(\frac{1}{30}\,\mathbb{Z} \cap [-0.1, 0.1]\right)\right\} \setminus \{(\pm 1, 0)\}, \\ X_2 \;&=\; \left\{(x,0) \mid x \in \frac{1}{30}\,\mathbb{Z} \cap [-2.5, 2.5] \setminus [-0.2, 0.2]\right\}, \end{aligned}$$

with $N = 964$ and $M = 151$ points, respectively, altogether $\tilde{N} = N + M = 1115$ points.

Figure 6, left, shows the function $s(x,v)$ which satisfies $c_1\|v\|^2 \leq s(x,v) \leq c_2\|v\|^2$ as well as $Ls(x,v)$, right, which approximates $-\|v\|^2$ well in the area $[-2.5, 2.5] \setminus [-0.2, 0.2]$. Figure 7 shows the collocation points, the area where $Ls(x,v) = 0$ (red) and the area where $s(x,v) = 0$ (blue), thus separating the area where it is a valid Finsler-Lyapunov function.

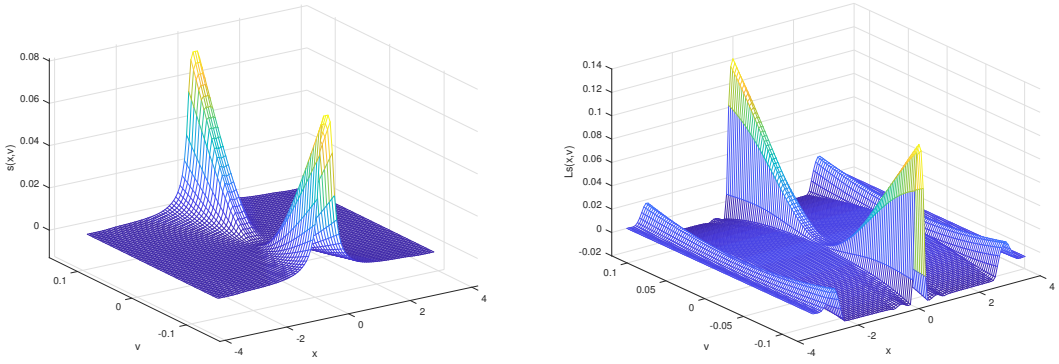

Figure 6: Example (28) with collocation points outside $[-0.2, 0.2]$. Left: The function $s(x, v)$, which is positive definite. Right: The function $Ls(x, v)$ which approximates $-\|v\|^2$ well outside $[-0.2, 0.2]$.

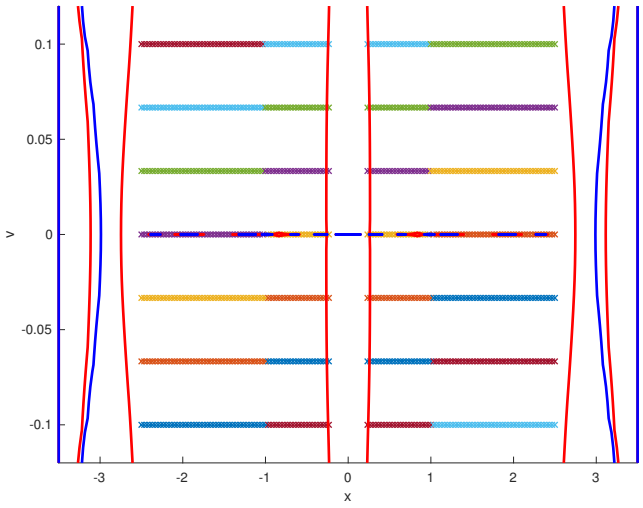

Figure 7: Example (23): The collocation points outside $[-0.2, 0.2]$ as well as the level sets $Ls(x, v) = 0$ (red) and $s(x, v) = 0$ (blue). Note that $Ls(x, v) < 0$ and $s(x, v) > 0$ hold in the area where the collocation points are placed, apart from $v = 0$.

Next we do not set any collocation points near the asymptotically stable equilibria at ± 1. In particular, we choose the collocation points

$$\begin{aligned} X_1 &= \left\{(x, v) \in \frac{1}{30}\mathbb{Z} \cap [-0.8, 0.8] \times \frac{1}{30}\mathbb{Z} \cap [-0.1, 0.1]\right\} \setminus \{(0, 0)\}, \\ X_2 &= \left\{(x, 0) \mid x \in \frac{1}{30}\mathbb{Z} \cap [-0.8, 0.8]\right\}, \end{aligned}$$

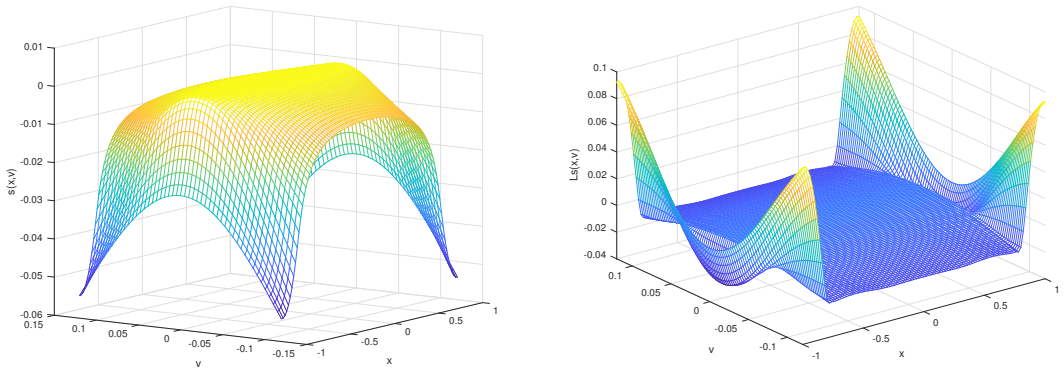

Figure 8: Example (28) with collocation points inside $[-0.8, 0.8]$. Left: The function $s(x, v)$, which is negative definite as the equilibrium at 0 is unstable. Right: The function $Ls(x, v)$ which approximates $-\|v\|^2$ well.

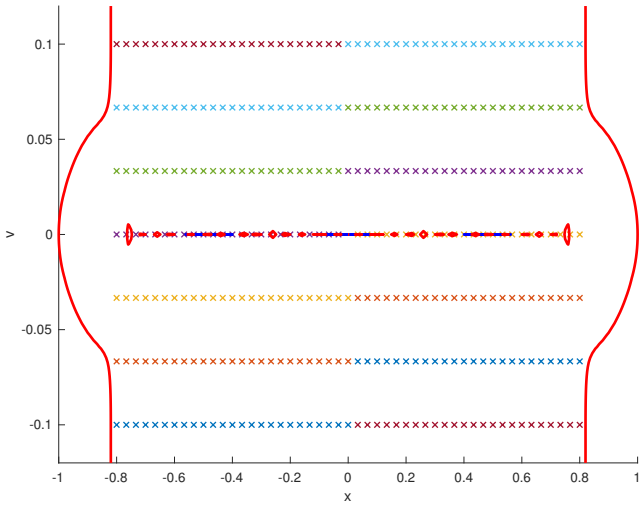

Figure 9: Example (23): The collocation points inside $[-0.8, 0.8]$ as well as the level sets $Ls(x, v) = 0$ (red) and $s(x, v) = 0$ (blue). Note that $Ls(x, v) < 0$ and $s(x, v) < 0$ hold in the area where the collocation points are placed, apart from $v = 0$, since the equilibrium at 0 is unstable.

with $N = 342$ and $M = 49$ points, respectively, altogether $\tilde{N} = N + M = 391$ points.

Figure 8, left, shows the function $s(x, v)$ which satisfies $-c_1\|v\|^2 \leq s(x, v) \leq -c_2\|v\|^2$ as well as $Ls(x, v)$, right, which approximates $-\|v\|^2$ well in the area $[-0.8, 0.8]$. Note that $s(x, v)$ is negative definite, indicating that the origin is an unstable equilibrium. Figure 9 shows the collocation points, the area where $Ls(x, v) = 0$ (red) and the area where $s(x, v) = 0$ (blue).

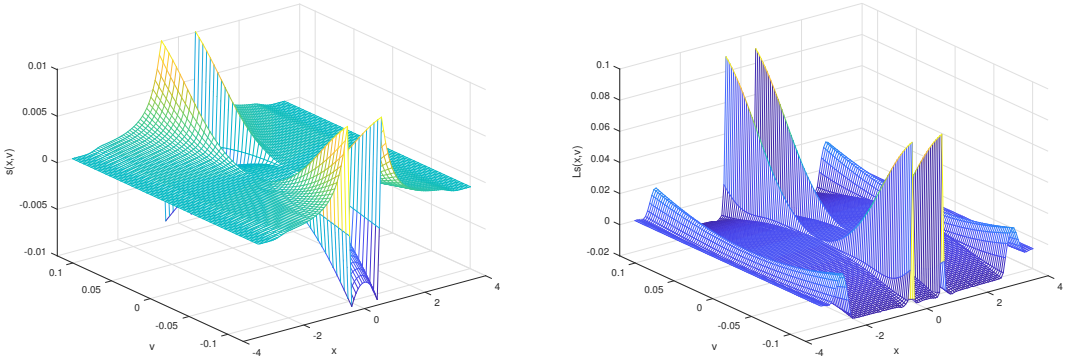

Figure 10: Example (28) with collocation points inside $[-2.5, 2.5] \setminus ([-0.55, -0.45] \cup [0.45, 0.55])$. Left: The function $s(x, v)$ is negative definite in $[-0.45, 0.45]$, and positive definite for $|x| > 0.55$. Right: The function $Ls(x, v)$ which approximates $-\|v\|^2$ well in all areas with collocation points.

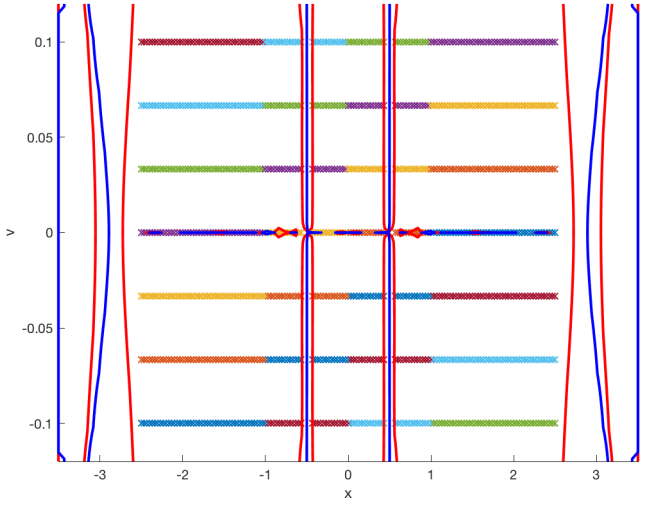

Figure 11: Example (23): The collocation points inside $[-2.5, 2.5] \setminus ([-0.55, -0.45] \cup [0.45, 0.55])$ with as well as the level sets $Ls(x, v) = 0$ (red) and $s(x, v) = 0$ (blue). $Ls(x, v)$ approximates $-\|v\|^2$ well in all areas, where the collocation points are placed. The sign of $s(x, v)$ shows whether it belongs to an area with stable or unstable equilibrium; it is positive for x between -2.5 and -0.5, negative for x between -0.5 and 0.5, and again positive for x between 0.5 and 2.5.

Finally, we take advantage of the fact that the equilibria do not play any special role in the construction of the function. We cut out two small intervals, one between -1 and

0, and one between 0 and 1. In each of the three remaining intervals, a function V exists, and we expect it to be positive definite in the two areas with the asymptotically stable equilibria ± 1 and negative definite in the area with the unstable equilibrium at 0. In particular, we choose the collocation points

$$\begin{aligned} X_1 &= \left\{(x,v) \in \left(\frac{1}{30}\mathbb{Z} \cap [-2.5, 2.5] \setminus ([-0.55, -0.45] \cup [0.45, 0.55])\right) \times \frac{1}{30}\mathbb{Z} \cap [-0.1, 0.1]\right\} \\ &\qquad\qquad \setminus \{(\pm 1, 0), (0, 0)\}, \\ X_2 &= \left\{(x,0) \mid x \in \frac{1}{30}\mathbb{Z} \cap [-2.5, 2.5] \setminus ([-0.55, -0.45] \cup [0.45, 0.55])\right\}, \end{aligned}$$

with $N = 1012$ and $M = 151$ points, respectively, altogether $\tilde{N} = N + M = 1163$ points.

Figure 10, left, shows the function $s(x, v)$ which is negative definite in $[-0.45, 0.45]$, including the unstable equilibrium, and positive definite outside $[-0.55, 0.55]$, reflecting the stability of the two asymptotically equilibria in this domain. Figure 10, right, shows $Ls(x, v)$ which approximates $-\|v\|^2$ well in the where the collocation points are placed. Figure 11 shows the collocation points, the area where $Ls(x, v) = 0$ (red) and the area where $s(x, v) = 0$ (blue).

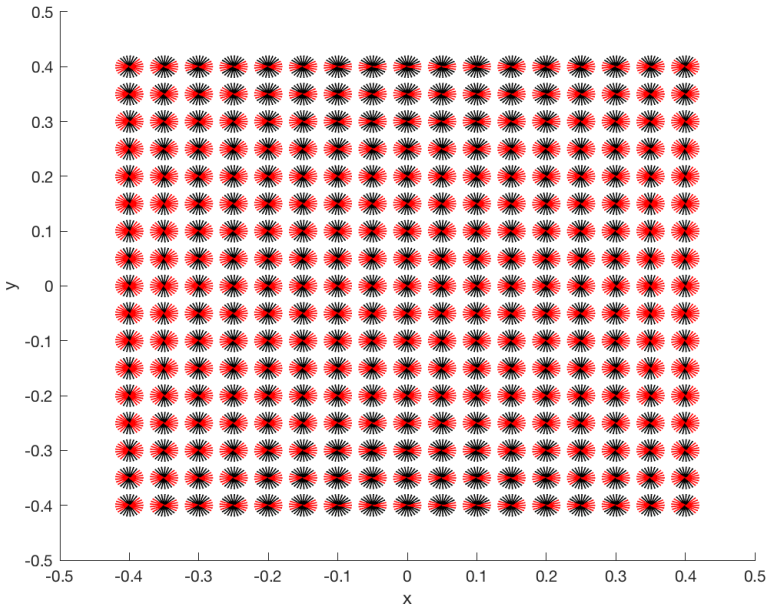

Figure 12: Example (29): At each point $\mathbf{x}$ the directions $\mathbf{v}$ are shown, where $Ls(\mathbf{x}, \mathbf{v}) < 0$; in this case all values are negative. The colours of the line in direction $\mathbf{v}$ at point $\mathbf{x}$ indicate the sign of $s(\mathbf{x}, \mathbf{v})$ at each point $\mathbf{x}$: the line is black where $s(\mathbf{x}, \mathbf{v}) > 0$, indicating a stable direction, and the line is red where $s(\mathbf{x}, \mathbf{v}) \leq 0$, indicating an unstable direction.

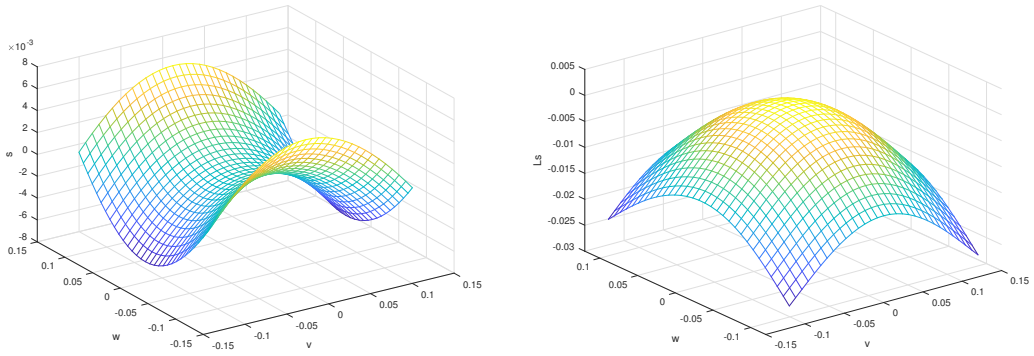

Figure 13: Example (29). Left: The function $s((0.16, 0.16), (v, w))$, showing the expected behaviour. Right: The function $Ls((0.16, 0.16), (v, w))$ which approximates $-\|(v, w)\|^2$ well. Note that no point $(\mathbf{x}_0, \mathbf{v})$ with $\mathbf{x}_0 = (0.16, 0.16)$ is a collocation point.

5.2 Two-dimensional linear example

We consider the two-dimensional, linear example

$$\left\{ \begin{array}{rcl} \dot{x} & = & x \\ \dot{y} & = & -y \end{array} \right. \tag{29}$$

with a saddle point at the origin.

We use the Wendland function $\psi_{5,2}(r) = (1-r)_+^7(16r^2 + 7r + 1)$ and the collocation points defined below containing $N = 2025$ and $M = 225$ points, respectively; altogether we have $\tilde{N} = N + M = 2250$ points.

$$\begin{aligned} X_1 &= \left\{ (\mathbf{x}, \mathbf{v}) \in [-0.5, 0.5]^2 \times \mathbb{R}^2 \mid x, y \in \frac{1}{14}\mathbb{Z}^2, \right. \\ &\qquad \left. \mathbf{v} \in \{0.1(\cos(\theta), \sin(\theta)), \theta = 2k\pi/9, k = 1, \ldots, 9\} \right\} \setminus \{(0,0)\}, \text{ and} \\ X_2 &= \left\{ (\mathbf{x}, 0) \in [-0.5, 0.5]^2 \times \mathbb{R}^2 \mid x, y \in \frac{1}{14}\mathbb{Z}^2 \right\}. \end{aligned}$$

$Ls(\mathbf{x}, \mathbf{v})$ is negative for all points $\mathbf{x} \in [-0.5, 0.5]^2$ and $\mathbf{v} \neq 0$ close to 0. Figure 12 shows at each point $\mathbf{x}$ the directions $\mathbf{v}$, where $s(\mathbf{x}, \mathbf{v}) > 0$ (black, stable directions) and $s(\mathbf{x}, \mathbf{v}) \leq 0$ (red, unstable directions). This is as expected since

$$s(\mathbf{x}, \mathbf{v}) = \frac{1}{2}\mathbf{v}^T \mathrm{diag}(-1, 1)\mathbf{v} = \frac{1}{2}(-v^2 + w^2), \tag{30}$$

where $\mathbf{v} = (v, w)$, is a solution of (14), see (27). Hence, the stable directions, where $s(\mathbf{x}, \mathbf{v}) > 0$, are $\mathbf{v} = (\cos(\theta), \sin(\theta))$ with $\theta \in \left(\frac{\pi}{4}, \frac{3\pi}{4}\right) \cup \left(\frac{5\pi}{4}, \frac{7\pi}{4}\right)$.

Figure 13 shows $Ls(\mathbf{x}_0, \mathbf{v})$ and $s(\mathbf{x}_0, \mathbf{v})$ as a function of $\mathbf{v}$ at a fixed point $\mathbf{x}_0 = (0.16, 0.16)$; note that no point $(\mathbf{x}_0, \mathbf{v})$ is a collocation point. $Ls(\mathbf{x}_0, \cdot)$ behaves like $-\|\mathbf{v}\|^2$

as expected since s was computed as the generalised interpolant of this data. s is close to the solution (30) described above.

5.3 Nine equilibria

Now we consider the two-dimensional example

$$\begin{cases} \dot{x} &= x(1-x^2) \\ \dot{y} &= -y(1-y^2) \end{cases} \tag{31}$$

with nine equilibria (x, y), $x, y \in \{-1, 0, 1\}$. The stability of the equilibria is as follows: $(\pm 1, 0)$ are asymptotically stable, $(0, \pm 1)$ are unstable with 2-dimensional unstable manifold, while the other 5 are saddle points. $(0, 0)$ has the stable manifold in direction of the y-axis, and the unstable manifold in direction of the x-axis, while for the remaining four equilibria $(\pm 1, \pm 1)$ the situation is the other way round.

For the computation we solve again the problem (14) using the Wendland function $\psi_{5,2}(r) = (1-r)_+^7(16r^2 + 7r + 1)$ and the collocation points defined below containing $N = 4761$ and $M = 729$ points, respectively; altogether we have $\tilde{N} = N + M = 5490$ points, shown in Figure 14, left. Note that there are no collocation points along the lines $x = \pm 0.5$ and $y = \pm 0.5$, separating the nine equilibria.

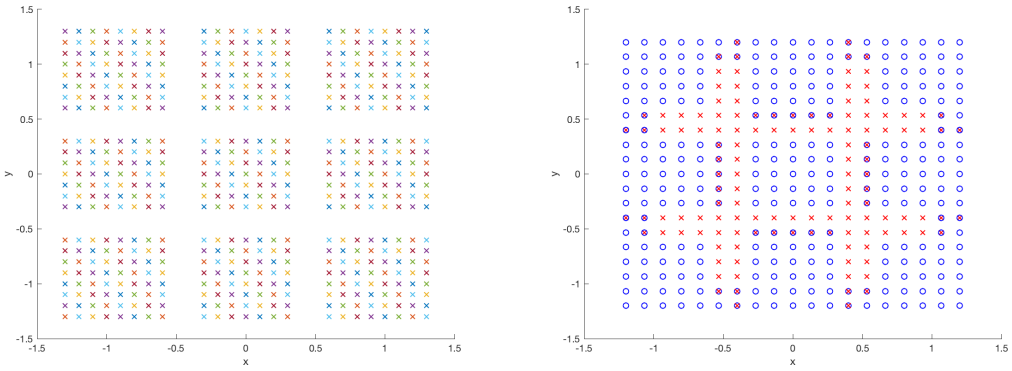

Figure 14: Example (31). Left: The collocation points X_1 in the (x, y)-plane; note that lines separating the nine equilibria do not contain collocation points. Right: Some points in the $\mathbf{x} = (x, y)$-plane, where the sign of $Ls(\mathbf{x}, \mathbf{v})$ is calculated: if the sign of $Ls(\mathbf{x}, \mathbf{v})$ is negative for a $\mathbf{v}$, then a blue circle is plotted, if the sign is non-positive for a $\mathbf{v}$, then a red cross is plotted. One can see the red crosses along the lines where no collocation points where placed.

$$\begin{aligned} X_1 &= \big\{(\mathbf{x}, \mathbf{v}) \in [-1.3, 1.3]^2 \times \mathbb{R}^2 \mid x, y \in 0.1 \cdot \mathbb{Z}^2, x, y \notin \{\pm 0.4, \pm 0.5\}, \\ &\qquad \mathbf{v} \in \{0.1(\cos(\theta), \sin(\theta)), \theta = 2k\pi/9, k = 1, \ldots, 9\}\big\}, \text{ and} \\ X_2 &= \{(\mathbf{x}, 0) \in [-1.3, 1.3]^2 \times \mathbb{R}^2 \mid x, y \in 0.1 \cdot \mathbb{Z}^2\}. \end{aligned}$$

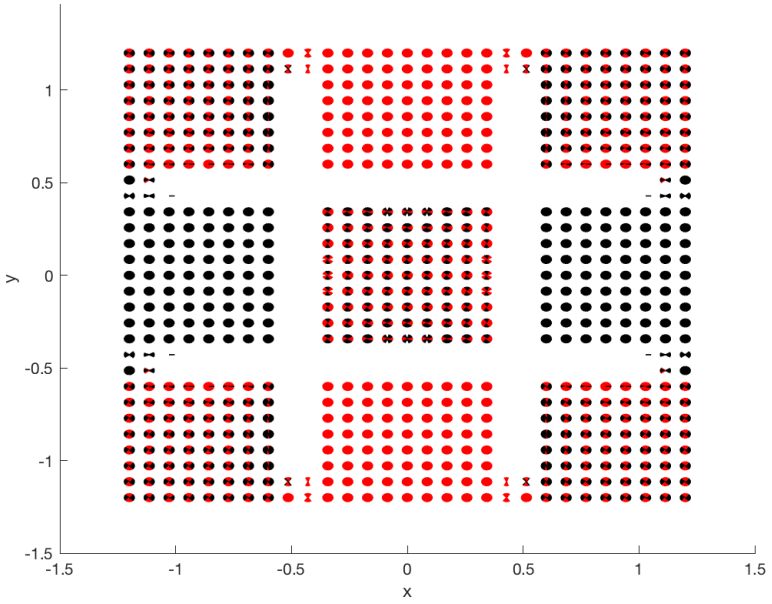

Figure 15: Example (31): At each point $\mathbf{x}$ the directions $\mathbf{v}$ are shown, where $Ls(\mathbf{x}, \mathbf{v}) < 0$. The colours of the line in direction $\mathbf{v}$ at point $\mathbf{x}$ indicate the sign of $s(\mathbf{x}, \mathbf{v})$ at each point $\mathbf{x}$: the line is black where $s(\mathbf{x}, \mathbf{v}) > 0$, indicating a stable direction, and the line is red where $s(\mathbf{x}, \mathbf{v}) \leq 0$, indicating an unstable direction.

Figure 14, right, shows points $\mathbf{x}$ where $Ls(\mathbf{x}, \mathbf{v})$ was evaluated for many $\mathbf{v} \neq 0$. For each $\mathbf{v}$ where $Ls(\mathbf{x}, \mathbf{v}) < 0$, a blue circle was plotted at the position $\mathbf{x}$, while for each $\mathbf{v}$ where $Ls(\mathbf{x}, \mathbf{v}) \geq 0$ a red cross was drawn at position $\mathbf{x}$. One can clearly see that the sign is negative except around the lines $x = \pm 0.5$ and $y = \pm 0.5$, where no collocation points where placed.

Figure 15 shows the sign of the stable and unstable directions $\mathbf{v}$ at each point $\mathbf{x}$ the directions $\mathbf{v}$, if $Ls(\mathbf{x}, \mathbf{v}) < 0$; otherwise, no line is plotted. The colour is determined by the sign of s: if $s(\mathbf{x}, \mathbf{v}) > 0$, then the direction is black (stable), and if $s(\mathbf{x}, \mathbf{v}) \leq 0$, then it is red (unstable directions). One can observe that in the areas around the nine equilibrium points, the directions are as expected by the stability. However, while the asymptotically stable and the unstable ones with a 2-dimensional unstable manifold show the stability in all points, the stable and unstable directions show more variation in the areas around the saddle points.

6 Discussion and conclusion

We have presented a method to numerically construct Finsler-Lyapunov functions, which show incremental stability of solutions of an ODE $\dot{x} = f(x)$, $x \in \mathbb{R}^n$. A Finsler-Lyapunov

function is a scalar-valued function with domain $(x, v) \in \mathbb{R}^n \times \mathbb{R}^n$, where x denotes a point in the phase space and v a point in the tangent space at x. We have proposed a linear first-order PDE with prescribed values at $v = 0$, and have approximately solved it using meshless collocation to construct a Finsler-Lyapunov function.

Finsler-Lyapunov functions can be used to show existence, uniqueness and stability of different types of attractors, such as equilibria or periodic orbits, and give information about their basins of attraction. Depending on the set of v for which the contraction condition holds, we can distinguish between different types of attractors. This can be implemented easily in the proposed method by choosing collocation points in the respective set.

We have shown existence results and error estimates in the case of exponentially stable equilibria and periodic orbits. Moreover, we have shown that the method can also be used to detect stable and unstable directions of unstable equilibria through the sign of the computed function in each direction v.

The error estimates show that the denser the collocation points, the smaller the error to an existing Finsler-Lyapunov function, and thus, from some threshold onwards, the constructed function is a Finsler-Lyapunov function itself.

In applications, the attractor and its basin of attraction are not known a priori. Hence, the error estimates, which assume that the collocation points are sufficiently dense and placed in the basin of attraction, do not serve to determine the density or position of the collocation points in practical examples. To apply the method, there are two approaches: either one places points in a small area, and then increases the area until the construction of a Finsler-Lyapunov function is unsuccessful. Or one starts with a large set and reduces it until the construction succeeds.

Regarding the density of the collocation points, the method is suitable for refinement: starting with a coarse set, collocation points are added in areas where the properties of a Finsler-Lyapunov function are not fulfilled. Summarising, the method gives information, when it succeeds to construct a Finsler-Lyapunov function, but if it fails, either the points are outside the basin of attraction or they were not sufficiently dense, and this has to be explored in more detail.

One advantage of Finsler-Lyapunov functions is that they do not require the location of the respective attractor. However, if several of them are present in the system, then we need to separate the areas between them. This is less restrictive than exactly locating attractors. Future work will include how to detect areas separating the different dynamics, where no collocation points should be placed. Moreover, we will extend the methodology to other, more complicated attractors.

Since the requirements for a Finsler-Lyapunov function are inequalities, it is robust with respect to perturbations of the system. The method is thus very well suited for generalisations to systems with uncertainties, such as ODEs where the constant coefficients are substituted by intervals or stochastic differential equations.

References

[1] Borg, G. *A condition for the existence of orbitally stable solutions of dynamical systems.* Kungliga Tekniska Högskolan Handlingar Stockholm 153, 1960.

[2] Buhmann, M. *Radial basis functions: theory and implementations*, vol. 12 of *Cambridge Monographs on Applied and Computational Mathematics.* Cambridge University Press, Cambridge, 2003.

[3] Forni, F., and Sepulchre, R. A differential Lyapunov framework for contraction analysis. *IEEE Trans. Autom. Control 59*, 3 (2014), 614–628.

[4] Giesl, P. On a matrix-valued PDE characterizing a contraction metric for a periodic orbit. submitted.

[5] Giesl, P. *Construction of Global Lyapunov Functions Using Radial Basis Functions.* Lecture Notes in Math. 1904, Springer, 2007.

[6] Giesl, P. Converse theorems on contraction metrics for an equilibrium. *J. Math. Anal. Appl. 424*, 2 (2015), 1380–1403.

[7] Giesl, P. Computation of a Finsler-Lyapunov function using meshless collocation. In *Mathematical and Numerical Aspects of Dynamical System Analysis* (2017), J. Awrejcewicz, M. Kazmierczak, J. Mrozowski, and P. Olejnik, Eds., DAB&M of TUL Press, pp. 193–204.

[8] Giesl, P., and Wendland, H. Meshless collocation: Error estimates with application to dynamical systems. *SIAM J. Numer. Anal. 45* (2007), 1723–1741.

[9] Hahn, W. *Stability of Motion.* Springer, Berlin, 1967.

[10] Hartman, P. *Ordinary Differential Equations.* Wiley, New York, 1964.

[11] Hartman, P., and Olech, C. On global asymptotic stability of solutions of differential equations. *Trans. Amer. Math. Soc. 104* (1962), 154–178.

[12] Krasovskiĭ, N. *Problems of the Theory of Stability of Motion.* Mir, Moskow, 1959. English translation by Stanford University Press, 1963.

[13] Leonov, G., Burkin, I., and Shepelyavyi, A. *Frequency Methods in Oscillation Theory.* Ser. Math. and its Appl.: Vol. 357, Kluwer, 1996.

[14] Lohmiller, W., and Slotine, J. E. On contraction analysis for non-linear systems. *Automatica 34*, 6 (1998), 683–696.

[15] Powell, M. J. D. The theory of radial basis function approximation in 1990. In *Advances in numerical analysis, Vol. II (Lancaster, 1990)*, Oxford Sci. Publ. Oxford Univ. Press, New York, 1992, pp. 105–210.

[16] Schaback, R., and Wendland, H. Kernel techniques: from machine learning to meshless methods. *Acta Numer. 15* (2006), 543–639.

[17] Stenström, B. Dynamical systems with a certain local contraction property. *Math. Scand. 11* (1962), 151–155.

[18] Wendland, H. Piecewise polynomial, positive definite and compactly supported radial functions of minimal degree. *Adv. Comput. Math. 4*, 4 (1995), 389–396.

[19] Wendland, H. *Scattered Data Approximation*, vol. 17 of *Cambridge Monographs on Applied and Computational Mathematics*. Cambridge University Press, Cambridge, 2005.